The EMBO Journal (2007) 26, 1487–1498 | © 2007 European Molecular Biology Organization | All Rights Reserved 0261-4189/07
www.embojournal.org

THE EMBO JOURNAL

Integrin-mediated adhesion orients the spindle parallel to the substratum in an EB1- and myosin X-dependent manner

Fumiko Toyoshima[1,2,*] and Eisuke Nishida[1]

[1]Department of Cell and Developmental Biology, Graduate School of Biostudies, Kyoto University, Sakyo-ku, Kyoto, Japan and [2]Precursory Research for Embryonic Science and Technology, JST, Honcho Kawaguchi, Saitama, Japan

The orientation of mitotic spindles is tightly regulated in polarized cells, but it has been unclear whether there is a mechanism regulating spindle orientation in nonpolarized cells. Here we show that integrin-dependent cell adhesion to the substrate orients the mitotic spindle of nonpolarized cultured cells parallel to the substrate plane. The spindle is properly oriented in cells plated on fibronectin or collagen, but misoriented in cells on poly-L-lysine or treated with the RGD peptide or anti-β1-integrin antibody, indicating requirement of integrin-mediated cell adhesion for this mechanism. Remarkably, this mechanism is independent of gravitation or cell–cell adhesion, but requires actin cytoskeleton and astral microtubules. Furthermore, myosin X and the microtubule plus-end-tracking protein EB1 are shown to play a role in this mechanism through remodeling of actin cytoskeleton and stabilization of astral microtubules, respectively. Our results thus uncover the existence of a mechanism that orients the spindle parallel to the cell–substrate adhesion plane, and identify crucial factors involved in this novel mechanism.

The EMBO Journal (2007) **26,** 1487–1498. doi:10.1038/sj.emboj.7601599; Published online 22 February 2007
Subject Categories: cell & tissue architecture; cell cycle
Keywords: cell–substrate adhesion; EB1; integrin; myosin X; spindle orientation

Introduction

Orientation of the mitotic spindle along the predetermined axis plays an important role in embryogenesis, neurogenesis, and asymmetric cell division. As was first recognized by Sachs, and later by Hertwig, a mitotic spindle tends to place itself in the center of a cell and the axis of the spindle typically lies in the longest axis of the cell (the rules of Sachs and Hertwig) (Wilson, 1925; Rappaport, 1996). Thus, the cell geometry should be one of a determinant for spindle orientation and positioning because this defines the center and the long axis of the cell.

*Corresponding author. Department of Cell and Developmental Biology, Graduate School of Biostudies, Kyoto University, Sakyo-ku, Kyoto 606-8502, Japan. Tel.: +81 75 753 9428; Fax: +81 75 753 4235;
E-mail: ftoyoshima@lif.kyoto-u.ac.jp

Received: 9 June 2006; accepted: 22 January 2007; published online: 22 February 2007

In polarized cells, such as cells in epithelial tissues, however, cortical cues, rather than cell geometry, strictly regulate spindle orientation. The epithelial cells divide either parallel or perpendicular to the epithelial plane. In each type of cell division, the dividing cells orient their mitotic spindle along the planar axis or the apical–basal axis, respectively (Lamprecht, 1990; Reinsch and Karsenti, 1994). In *Drosophila* neuroectoderm, adherens junctions are crucial for the spindle orientation along the planar axis (Lu *et al*, 2001). Mammalian cultured MDCK cells, which develop apico–basal polarity and form the epithelial-like sheet of monolayer, maintain tight junctions throughout mitosis (Reinsch and Karsenti, 1994). Interaction of astral microtubules with cortical factors is important for spindle orientation and positioning in polarized cells. This interaction is mediated by a protein family, so called +Tips, which includes EB1, adenomatous polyposis coli (APC) tumor suppressor, and dynein (Schuyler and Pellman, 2001; Mimori-Kiyosue and Tsukita, 2003; Gundersen *et al*, 2004). It is believed that cell–cell adhesion provides a cortical planar cue to orient the mitotic spindle parallel to the epithelial plane by regulating the interaction of astral microtubules with cortex in a +Tips-dependent manner (Bienz, 2001).

In nonpolarized cultured cells, it is reported that the spindle orients along the long cell axis and is positioned in the center of the cell in accordance with the rules of Sachs and Hertwig, in a +Tips-dependent manner (O'Connell and Wang, 2000; Rogers *et al*, 2002; Green and Kaplan, 2003). Thus, cell shape might be a determinant for spindle orientation and positioning in nonpolarized cultured cells. These mechanisms may ensure that the cytokinesis occurs along the short axis of the cells and that the size of two daughter cells should be same. When nonpolarized adherent cells, such as HeLa cells, are plated on a culture dish, they proliferate and divide on the surface of the dish, leading to formation of the sheet of cell monolayer. However, there has been no study investigating how the orientation of this anchorage-dependent cell division is regulated. In this study, we have found that the mitotic spindles are oriented along the axis parallel to the cell–substrate adhesion plane in nonpolarized cells. In contrast to the spindle orientation in polarized epithelial cells, which depends on cell–cell adhesion, this mechanism is independent of cell–cell adhesion, but dependent on integrin-mediated cell–substrate adhesion. This mechanism requires EB1 and myosin X, which are involved in stabilization of astral microtubules and actin reorganization during mitosis, respectively. Our results reveal the novel mechanism for spindle orientation that orients the spindle along the axis parallel to the cell–substrate adhesion plane in nonpolarized adherent cells. This mechanism for spindle orientation may ensure that both daughter cells remain attached to the substrate after cell division, and thus could contribute to the anchorage-dependent proliferation of adherent cells.

Results

Mitotic spindles are oriented parallel to the substrate surface

In our microscopic observation of normal mitosis of HeLa cells on a coverslip, both spindle poles in a spindle were on the same focal plane, indicating the orientation of the spindle parallel to the surface of the coverslips. However, when the cells were released from the nocodazole-induced prometaphase arrest, the two spindle poles in a spindle were often on a different focal plane owing to the alignment of the mitotic spindle along the axis tilted to the surface of the coverslip (see Figure 1B). This observation prompted us to examine the possibility that there is a mechanism that orients the spindle parallel to the substrate surface in nonpolarized cells such as HeLa cells. To examine the spindle orientation in HeLa cells, *Z*-stack images were taken from 0.5 μm-thick sections of metaphase cells, which were immunostained with anti-γ-tubulin, anti-α-tubulin antibodies, and Hoechst (Figure1A, right), and the linear distance and the vertical distance between the two poles of the metaphase spindles (Figure 1A, left, *X* μm and *Y* μm, respectively) was measured.

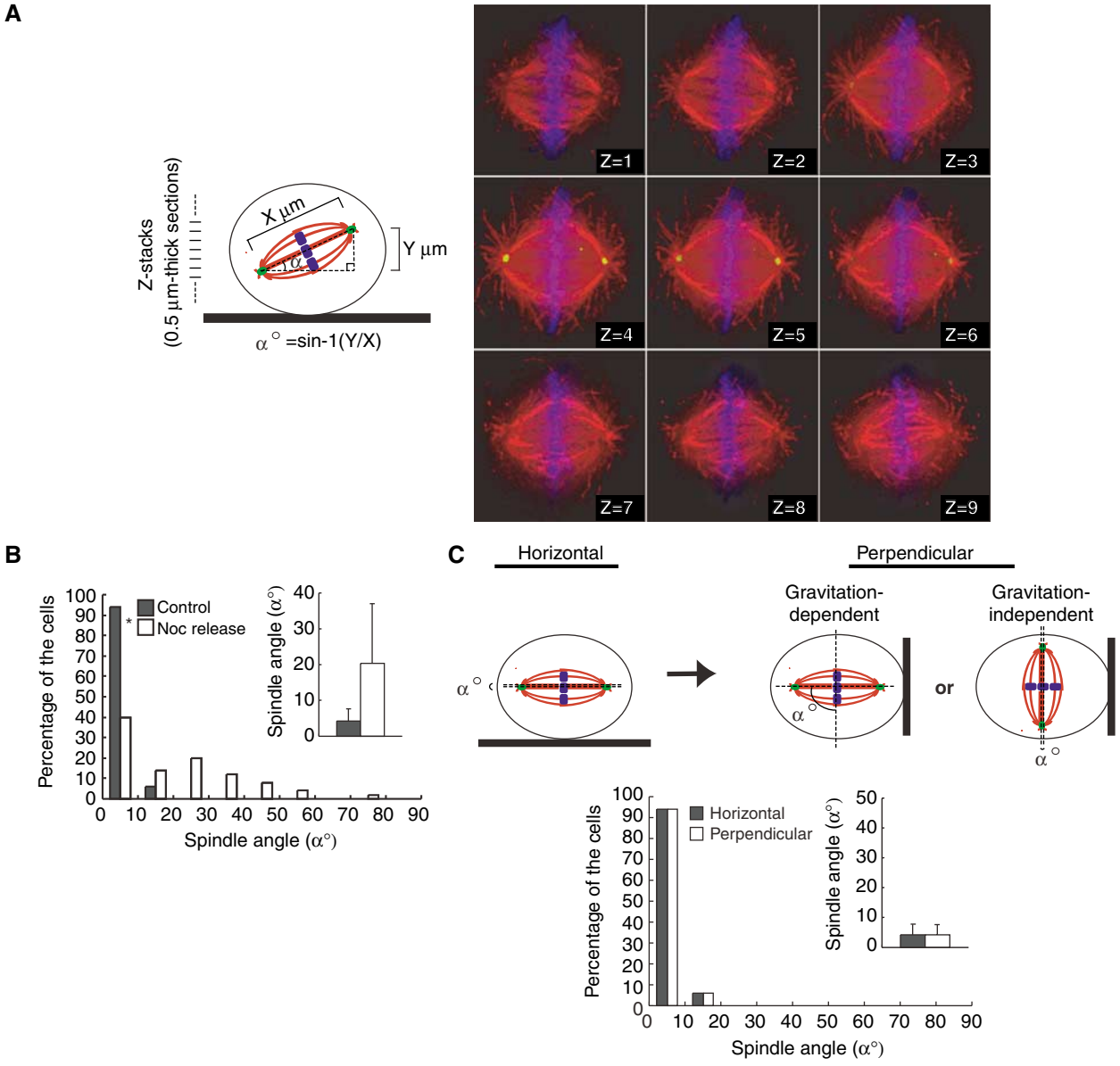

Figure 1 Mitotic spindles are oriented parallel to the substrate surface. (**A**) The spindle orientation analysis. The linear distance (left, *X* μm) and the vertical distance (left, *Y* μm) between the two poles of the metaphase spindles was measured by taking *Z*-stack images from 0.5 μm-thick sections of a metaphase cell, which was plated on a fibronectin-coated coverslip, synchronized in M phase, and immunostained with α-tubulin (red), anti-γ-tubulin (green), and Hoechst (blue) (right). The angle (spindle angle) between the axis of a metaphase spindle and that of substrate surface (left, α°) was calculated with inverse trigonometric function (left). (**B**) Distribution of spindle angles in control cells and the cells released from the nocodazole arrest. Metaphase cells were classified in terms of the spindle angle, and the percentages of each categories are shown in a histogram ($n=50$). The inset graph shows the average spindle angles (mean ± s.d.; $n=50$). *$P<0.005$, as compared with the control, analyzed by *F*-test. (**C**) HeLa cells were plated on a fibronectin-coated coverslip and were synchronized in S phase by a double-thymidine block. Immediately after the release, the coverslip was kept horizontal or set up perpendicularly, incubated for 10 h, and then fixed (upper). Distribution (histogram; $n=50$) and the average (inset; mean ± s.d.; $n=50$) of spindle angles are shown (bottom).

Then, the angle between the axis of a metaphase spindle and that of the substrate surface (Figure 1A, left, α°, which is termed the spindle angle) was calculated. We confirmed that cells were in metaphase when their chromosomes were aligned on a metaphase plate. We analyzed 50 metaphase cells in each condition and found that the spindle angle falls within 10° in more than 90% of the control cells, but in less than 40% of the cells, which were released from the nocodazole arrest (Figure 1B). The average spindle angles were 4.2° and 20.4°, respectively, in control cells and the cells released from the nocodazole arrest. Therefore, the spindle is oriented parallel to the substrate surface in control cells but severely misoriented in cells released from the nocodazole arrest. If spindle orientation depends on gravitation, the spindle angle should be increased when a coverslip (that is, the substrate surface) is set up perpendicularly. The result showed that the spindle angle was not increased at all when a coverslip was set up perpendicularly (Figure 1C), indicating that the spindle orientation is independent of gravitation.

Integrin-mediated cell–substrate adhesion is required for the spindle orientation parallel to the substrate surface

In polarized epithelial cells, cell–cell adhesion provides a planar cue to orient the spindle parallel to the epithelial plane (Bienz, 2001; Lu *et al*, 2001). To investigate whether cell–cell adhesion is required for proper spindle orientation in HeLa cells, synchronized HeLa cells were diluted enough to avoid cell–cell adhesion and plated on a fibronectin-coated coverslip (Figure 2A, left). Sparse cultures as well as semi-confluent cultures showed the properly oriented spindle parallel to the substrate surface (Figure 2A, right), indicating that cell–cell adhesion is not required for proper spindle orientation in HeLa cells. We then examined possible requirement of cell–substrate adhesion for spindle orientation. To test this, synchronized HeLa cells were plated on a coverslip coated with poly-L-lysine, an artificial substrate which does not bind to integrin (Machesky and Hall, 1997) or fibronectin or collagen, both of which are integrin-binding extracellular matrix components and facilitate integrin-dependent cell–substrate adhesion. The spindles were properly oriented in cells on fibronectin or collagen, but misoriented in cells on poly-L-lysine; the average spindle angles were 9.7°, 3.6°, and 17.7°, respectively, in cells on fibronectin, collagen, and poly-L-lysine (Figure 2B, left). The average spindle length was 13.2 μm in the cells on fibronectin. The spindle lengths were hardly changed in the cells on each substrate; 5.7% increase and 8.4% decrease, respectively, in cells on collagen and poly-L-lysine, compared to that in cells on fibronectin (Supplementary Figure S1A). To examine whether the effects on spindle angle are owing to indirect effects of spread basal area, we compared the spindle angle in the cells that spread to equal extents on poly-L-lysine, fibronectin, and collagen (Figure 2, upper right), by measuring both the spindle angle and the basal area of each metaphase cell. We analyzed 50 metaphase cells in each condition. The result showed that the spindles were properly oriented in cells that spread to equal extents on fibronectin or collagen, but misoriented in cells on poly-L-lysine (Figure 2B, bottom right), indicating that the effects on spindle angle are not due to indirect effects of spread basal area. When HeLa cells were plated on fibronectin in the presence of the RGD peptide, which is known to inhibit integrin–fibronectin interaction (Pierschbacher and Ruoslahti, 1984; Yamada and Kennedy, 1984), or a control RAD peptide, spindles were severely misoriented in the presence of the RGD peptide, but not in the presence of a control peptide (Figure 2C, left), even when the cells were spread to equal extents on fibronectin (Figure 2C, middle). The RGD peptide treatment hardly changed the spindle length, compared to the control RAD peptide (8.8% increase) (Supplementary Figure S1B). To examine the effect of cell width on the spindle orientation, we measured the cell length along the long cell axis at midsection in metaphase cells. No statistically significant difference in the average cell length at midsection was observed between the cells treated with the RGD peptide and a control peptide (Figure 2C, right), indicating that the effect of the RGD peptide on spindle angle is not due to indirect effect of cell width. Treatment with anti-β1 integrin antibody, which inhibits integrin-mediated adhesion (Wang *et al*, 2003), but not with the blocking antibodies against β3 integrin or αVβ6-integrin, both of which also bind fibronectin, resulted in misorientation of the spindles in the cells on fibronectin (Figure 2D). Downregulation of β1 integrin by siRNA also resulted in severe misorientation of spindles (Figure 2E). Treatment with anti-β1 integrin antibody and β1 integrin siRNA hardly changed the spindle length, compared to the controls (9 and 3% decrease, respectively) (Supplementary Figure S1C and D). To test whether the integrin-dependent mechanism for spindle orientation exists in nontransformed cells, we used NRK cells. As in HeLa cells, the spindles were properly oriented in NRK cells on fibronectin both in the presence and absence of cell–cell adhesion (Figure 2F). When the cells were plated on fibronectin, in the presence of the RGD peptide, the spindles were severely misoriented, but not in the presence of RAD peptide (Figure 2G). These results demonstrate that integrin-mediated cell–substrate adhesion is required for the proper spindle orientation in both HeLa cells and nontransformed NRK cells. Moreover, the time-lapse images of HeLa cells expressing histone 2B fused to green fluorescent protein (GFP-H2B) showed that the cells cultured in three dimensions by totally embedding the cells in a gel of reconstituted basement membrane matrix displayed random spindle orientation and separated their chromosomes along the axis of their spindles oriented randomly (Figure 3A and B, 3-D, and Supplementary Movie 2, 3, and 4), whereas the cells cultured on top of a matrix gel oriented their spindles parallel to the substratum (Figure 3A and D, 2-D and Supplementary Movie 1), indicating that the cell–substrate-adhesion-dependent mechanism for spindle orientation is functioning in cells in a three-dimensional situation.

Actin cytoskeleton is required for the spindle orientation parallel to the substrate surface

Integrin couples extracellular matrix with actin cytoskeleton and plays an important role in reorganization of actin architecture (Geiger *et al*, 2001; DeMali *et al*, 2003). To examine involvement of actin cytoskeleton in the spindle orientation, synchronized HeLa cells in G2 phase, which were plated on fibronectin, were treated with latrunculin B (Lat B), an inhibitor of actin polymerization (Spector *et al*, 1983). The spindles were misoriented in cells treated with Lat B; the spindle orientation became almost random (Figure 4A, left). Essentially the same degree of the spindle misorientation was

observed in cells treated with cytochalasin D (data not shown). The treatment with Lat B hardly changed the spindle length (0.8% increase, compared to the cells treated with DMSO) (Supplementary Figure S1E). To examine the effect of cell height on the spindle orientation, we measured the cell height by taking *Z*-stack images from 0.5 μm-thick sections of metaphase cells, which were stained with DHCC to visualize plasma membranes. The normalized values for the average

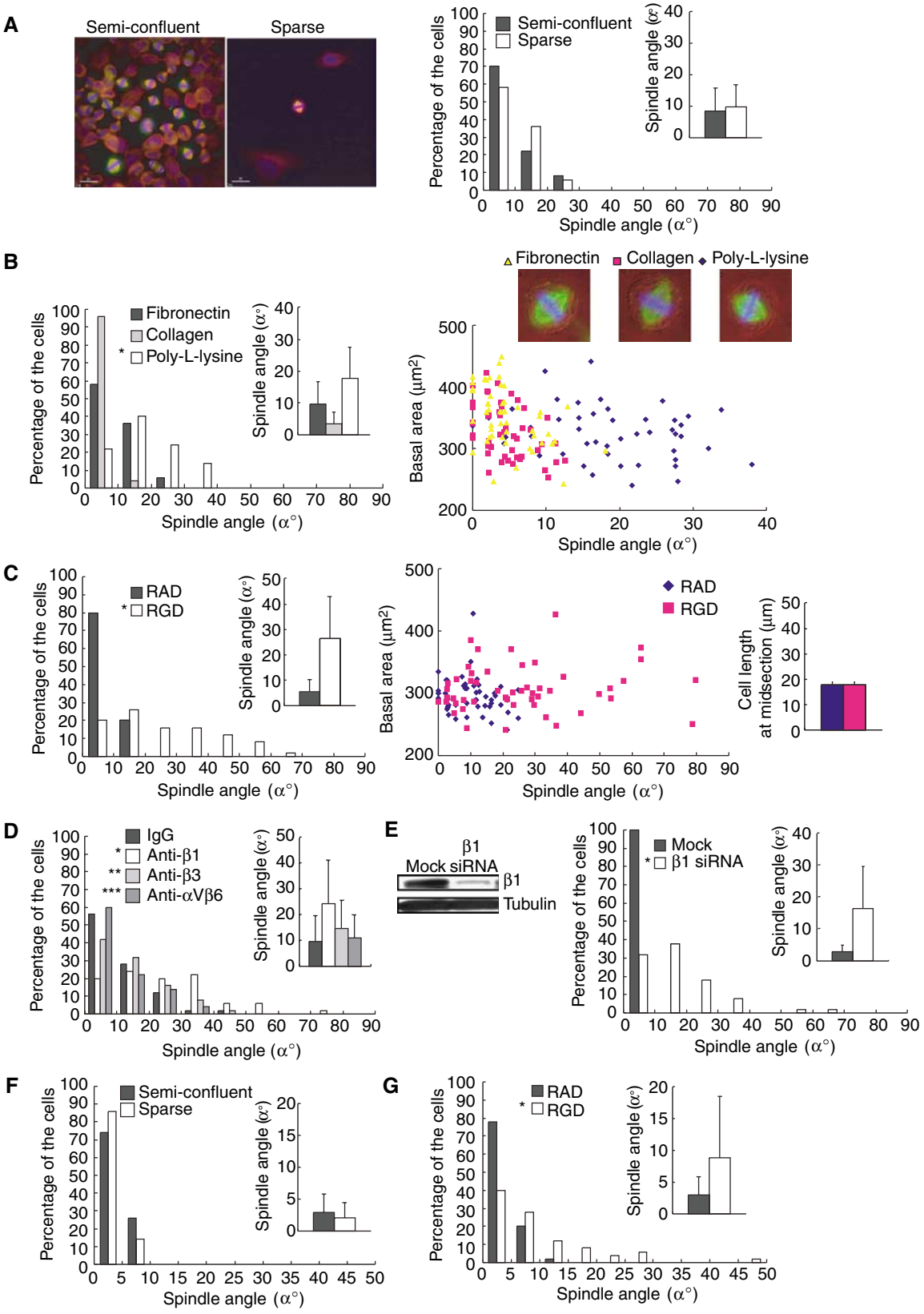

spindle angle per the average cell height were 1.0, 1.4, and 5.2, respectively, in control, DMSO-treated, and Lat B-treated cells (Figure 4A, middle). The spindles were properly oriented in cells that spread to equal extents on fibronectin in control and DMSO-treated cells, but misoriented in Lat B-treated cells (Figure 4A, right). The Lat B treatment hardly changed the average cell length at midsection of the metaphase cells (Figure 4A, right, inset). Thus, the effect of Lat B-treatment on spindle angle is not due to indirect effects of cell height, spread basal area, or cell width. Next, synchronized HeLa cells in M phase, which were obtained by incubating prometaphase cells with MG132, a proteasome inhibitor (Kisselev and Goldberg, 2001), were treated with Lat B. This also induced spindle misorientation (Figure 4B). This result indicates that disruption of actin cytoskeleton even after the mitotic entry is able to induce spindle misorientation. Astral microtubules and kinetochore microtubules appeared to be normally formed in Lat B-treated cells (data not shown). To further show the integrity of spindle assembly in Lat B-treated cells, localization of BubR1 was investigated with anti-BubR1 antibody. BubR1 is known to localize to kinetochores unattached to microtubules and dissociate from kinetochores when microtubules attach to kinetochores (Hoffman *et al*, 2001). Thus, BubR1 localizes to kinetochores during prometaphase and dissociates at metaphase. In Lat B-treated cells, BubR1 localized to the kintochores during prometaphase, and its kintochore localization was lost at metaphase (Supplementary Figure S2). This behavior of BubR1 is normal, indicating that the spindle assembly of the misoriented spindle in Lat B-treated cells is intact. The

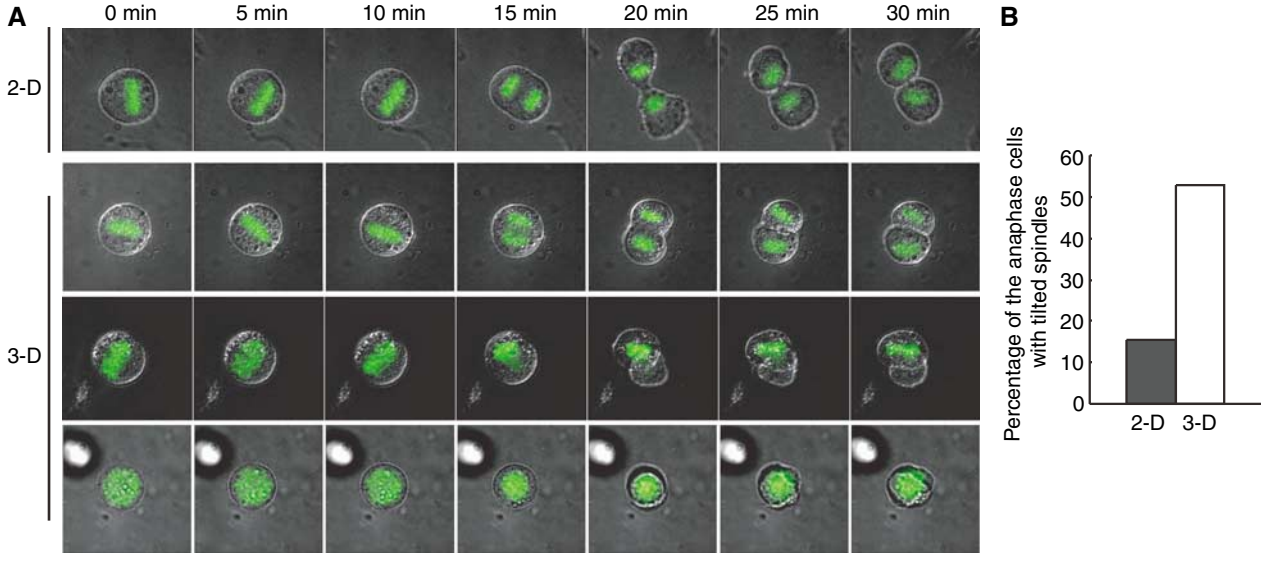

Figure 3 The cell–substrate adhesion regulates spindle orientation in the cells cultured in three dimensions. (**A**) Time-lapse images of the mitotic GFP-H2B-expressing HeLa cells that were cultured on top of (2-D) or within (3-D) a gel of a basement membrane matrix. The merge images of phase contrast and GFP-H2B are shown. For 3-D culture, three typical images of the cells are shown; the axes of the spindles were parallel (3-D, upper), tilted (3-D, middle), or perpendicular (3-D, bottom) to the horizontal plane. (**B**) Percentage of the cells that separate their chromosomes along the axis of their spindles which is tilted or perpendicular to the horizontal plane (2-D; $n=72$, 3-D; $n=34$).

Figure 2 Integrin-mediated cell–substrate adhesion is required for the spindle orientation parallel to the substrate surface. (**A**) Synchronized HeLa cells were plated on the fibronectin-coated coverslips immediately after the release from a double-thymidine block with dilution by 10 (Sparse) or without dilution (semiconfluent), incubated for 10 h, and subjected to the spindle orientation analysis (right, histogram; $n=50$, inset; mean$\pm$s.d.; $n=50$). The images of the cells stained with anti-α-tubulin antibody (red), anti-γ-tubulin antibody (green), and Hoechst (blue) are shown in the left. In sparse culture, the spindle angles were measured in cells that had no cell–cell contacts. (**B**) Synchronized HeLa cells were diluted by 10, and plated on the coverslips coated with fibronectin, collagen, or poly-L-lysine, and subjected to the spindle orientation analysis (left, histogram; $n=50$, inset; mean$\pm$s.d.; $n=50$). $^{*}P<0.025$, as compared with fibronectin, analyzed by *F*-test. Spindle angles were plotted as a function of basal area (right bottom, $n=50$). The merge images of phase contrast, α-tubulin (green), and Hoechst (blue) of a metaphase cell on each substrate are shown in the right upper. (**C**) Synchronized HeLa cells were plated on the fibronectin-coated coverslip without dilution in the presence of the GRGDNP peptide (RGD) or the GRADSP peptide (RAD), and subjected to the spindle orientation analysis (left, histogram; $n=50$, inset; mean$\pm$s.d.; $n=50$). $^{*}P<0.005$ as compared with controls RAD, analyzed by *F*-test. Spindle angles were plotted as a function of basal area (middle, $n=50$). The average cell width at midsection of metaphase cells was measured (right, mean$\pm$s.d.; $n=50$). (**D**) Synchronized HeLa cells were plated on the fibronectin-coated coverslip without dilution in the presence of mouse IgG, or adhesion-blocking antibodies against β1 integrin, β3 integrin, or αVβ6 integrin, and subjected to the spindle orientation analysis (histogram; $n=50$, inset; mean$\pm$s.d.; $n=50$). $^{*}P<0.001$, $^{**}P=0.59$, and $^{***}P=0.46$ as compared with control IgG, analyzed by *F*-test. (**E**) Synchronized HeLa cells on fibronectin were transfected with or without β1-integrin siRNA, and subjected to the spindle orientation analysis (right, histogram; $n=50$, inset; mean$\pm$s.d.; $n=50$). $^{*}P<0.001$ as compared with mock, analyzed by *F*-test. Cell lysates were prepared and analyzed by Western blotting with anti-β1 integrin (left, upper) and anti-α-tubulin (left, bottom) antibodies. (**F**) Synchronized NRK cells were plated on the fibronectin-coated coverslips immediately after the release from an aphidicolin block with dilution by 10 (Sparse) or without dilution (semiconfluent), incubated for 8 h, and subjected to the spindle orientation analysis (histogram; $n=50$, inset; mean$\pm$s.d.; $n=50$). In sparse culture, the spindle angles were measured in cells that had no cell–cell contacts. (**G**) Synchronized NRK cells were plated on the fibronectin-coated coverslip without dilution in the presence of the GRGDNP peptide (RGD) or the GRADSP peptide (RAD), and subjected to the spindle orientation analysis (histogram; $n=50$, inset; mean$\pm$s.d.; $n=50$). $^{*}P<0.005$, as compared with control RAD, analyzed by *F*-test.

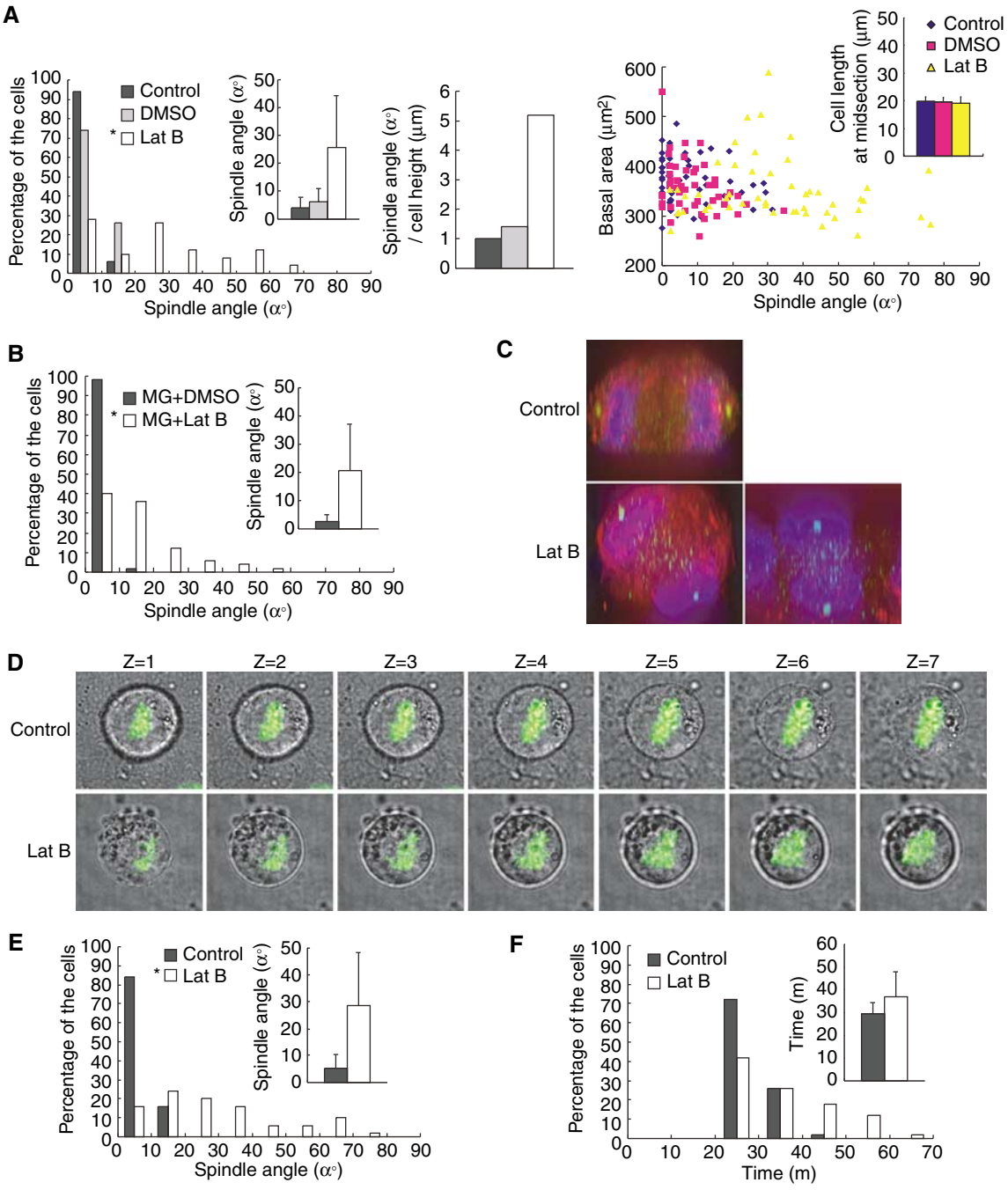

Figure 4 Actin cytoskeleton is required for the spindle orientation parallel to the substrate surface. (**A**) Synchronized HeLa cells on finronectin were treated with or without Lat B or DMSO, and subjected to the spindle orientation analysis (left, histogram; $n=50$, inset; mean±s.d.; $n=50$). $^*P<0.005$, as compared with DMSO, analyzed by *F*-test. The normalized values for the average spindle angle per the average cell heights were measured (middle, $n=50$). Spindle angles were plotted as a function of basal area (right, $n=50$). The average cell width at midsection of metaphase cells were measured (right inset, mean±s.d.; $n=50$) (**B**) HeLa cells on fibronectin were synchronized in M phase by incubating prometaphase cells with MG132, treated with or without Lat B or DMSO for 20 min, and subjected to the spindle orientation analysis (histogram; $n=50$, inset; mean±s.d.; $n=50$). $^*P<0.005$, as compared with DMSO, analyzed by *F*-test. (**C**) The *X*–*Z* projections from the *Z*-stack images of 20 focal planes (1 μm apart) from an untreated anaphase cell (upper) and Lat B-treated anaphase cells (bottom two panels). (**D**) *Z*-stack images of seven focal planes (1 μm apart) from an untreated cell in metaphase (Control) and a Lat B-treated cell in metaphase (Lat B). The merge images of phase contrast and GFP-H2B are shown. (**E**) Synchronized NIH 3T3 cells on fibronectin were treated with or without Lat B and subjected to the spindle orientation analysis (histogram; $n=50$, inset; mean±s.d.; $n=50$). $^*P<0.005$, as compared with the control, analyzed by *F*-test. (**F**) Distribution of (histogram; $n=50$) and the average (inset; mean±s.d.; $n=50$) time taken from the beginning of chromosome condensation to the onset of chromosome separation in HeLa cells that were treated with or without Lat B.

Lat B-treated cells were also able to separate their chromosomes along the axis of their spindle even when the spindle axis was tilted or perpendicular to the substrate surface (Figure 4C, Lat B). This clearly demonstrates that the misoriented spindle in the Lat B-treated cells is functionally intact. To eliminate the possibility that the tilt of the spindle

in Lat B-treated cells is an artefact resulting from experimental procedures such as fixation, we performed time-lapse observations of live cells. Three-dimensional time-lapse images of the HeLa cells expressing GFP-H2B were obtained by taking *Z*-stack images from 2 μm-thick sections every 3 min (Figure 4D and Supplementary Movie 5 and 6). In Lat B-untreated control cells, chromosomes (GFP-H2B) were positioned at the center of the cell on all the focal planes in metaphase (Figure 4D, Control). In contrast, in a Lat B-treated cell shown here, the focal point of the GFP-H2B images was on the bottom right side of the cell in $Z=1$ and shifting to the upper left side of the cell in $Z=7$ on the series of *Z*-sections in metaphase (Figure 4D, Lat B), indicating that the spindle was tilted. It should be noted that both Lat B-treated and untreated cells remained attached to the substrate during mitosis (Supplementary Movie 5 and 6). Therefore, the tilt of the spindle in Lat B-treated cells is not an artefact. The onset of anaphase was hardly delayed in Lat B-treated cells compared to that in control cells; the average times taken from the beginning of chromosome condensation to the onset of chromosome separation were 29.3 and 36.9 min, respectively, in control and Lat B-treated cells (Figure 4F). Moreover, the spindles did not align, then carried on through anaphase without proper orientation in Lat B-treated cells (Supplementary Movie 6). These results taken together clearly demonstrate that actin cytoskeleton is required for proper spindle orientation in HeLa cells and that disruption of actin cytoskeleton specifically results in misorientation of the spindle without deteriorating the function and the integrity of the mitotic spindle. Moreover, our result shows that Lat B treatment induced severe misorientation of spindles in NIH 3T3 fibroblasts (Figure 4E) as well as in HeLa cells, which are derived from epithelium, suggesting that this mechanism for spindle orientation is functioning in both epithelial cells and fibroblasts.

Astral microtubules and EB1 are required for the spindle orientation parallel to the substrate surface

Association of astral microtubules with cortical factors by a 'search-and-capture' mechanism (Kirschner and Mitchison, 1986) is important for spindle positioning, and this association is mediated by a protein family, so called +Tips (Schuyler and Pellman, 2001; Mimori-Kiyosue and Tsukita, 2003; Gundersen *et al*, 2004). To examine the role of astral microtubules in the spindle orientation parallel to the substrate surface, we treated NRK cells on fibronectin with nocodazole at the concentration of 10 ng/ml. At this concentration of nocodazole, astral microtubules were disrupted, whereas spindle microtubules were intact (data not shown), as reported previously (O'Connell and Wang, 2000). This treatment resulted in severe misorientation of spindles (Figure 5A, left). In NRK cells, Lat B treatment also induced severe misorientation of spindles, as in HeLa cells (Figure 5A, left). The normalized values for the average spindle angle per the average cell height were 1.0, 11.1, 6.0, respectively, in control, Nocodazle-treated, and Lat B-treated cells (Figure 5A, right). Therefore, astral microtubules as well as actin cytoskeleton are required for the proper spindle orientation. We then downregulated EB1 protein by siRNA in HeLa-S3 cells on fibronectin (Figure 5B, upper). EB1 protein, a member of +Tips, has an important role in microtubule dynamics and microtubule–F-actin interaction in many systems (Tirnauer and Bierer, 2000; Schuyler and Pellman, 2001; Mimori-Kiyosue and Tsukita, 2003; Gundersen *et al*, 2004). Downregulation of EB1 resulted in severe misorientation of spindles (Figure 5B, bottom). To confirm that the effect of EB1 siRNA on spindle orientation results from the knockdown of EB1 protein, rather than unspecific effects of the used RNA duplexes, we transfected EB1 siRNA-treated cells with a rescue construct (GFP-EB1-res) which encodes a GFP fusion of EB1 and is resistant to the siRNA owing to silent substitutions in the siRNA target region. Expression of GFP-EB1-res, but not GFP alone, could restore the proper spindle orientation in EB1 siRNA-transfected cells (Figure 5C), confirming the requirement of EB1 for proper spindle orientation. To exclude the effect of alteration of the matrix during the long-term incubation of the cells during transfection (72 h), synchronized HeLa cells transfected with or without EB1 siRNA were plated on fibronectin and incubated for 10 h. This also induced spindle misorientation in EB1 siRNA-transfected cells but not in mock cells (Figure 5D). EB1 siRNA slightly enhanced the misorientation of the spindle in cells on poly-L-lysine (Figure 5D), suggesting that EB1 may have an integrin-independent function in orientation of the spindle. In the EB1 siRNA-treated metaphase cells, astral microtubules were drastically reduced (Figure 5E), and spindles were shortened (14.3% decrease) (Supplementary Figure S1F) as reported previously in *Drosophila* S2 cells (Rogers *et al*, 2002; Goshima *et al*, 2005). Moreover, the time-lapse images of GFP-H2B-expressing HeLa cells that are transfected with EB1 siRNA show that one of the two daughter cells with misoriented spindles fails to maintain connection to the substratum after cell division (Figure 5F and Supplementary Movie 7). A similar phenotype was observed in the cells released from the nocodazole arrest (Figure 5G and Supplementary Movie 8), and the cells on fibronectin in the presence of β1 integrin antibody (Figure 5H and Supplementary Movie 10), in which spindles were misoriented (see Figures 1B and 2D). These results demonstrate that EB1 and astral microtubules are necessary for the integrin-dependent mechanism orientating spindles parallel to the substrate plane, and suggest that one of the important roles for EB1 in this mechanism is to promote the stabilization of astral microtubules. This mechanism ensures that both daughter cells remain attached to the substratum after cell division.

Myosin X is required for the spindle orientation parallel to the substrate surface and actin reorganization during M phase

Finally, we addressed the possible involvement of myosin in this novel mechanism for spindle orientation. We first examined the role of myosin II, which has an important role in cytokinesis and spindle assembly in mammalian cells (Robinson and Spudich, 2004; Rosenblatt *et al*, 2004). We used two drugs, Y-27632 and blebbistatin, to inactivate myosin II. Y-27632 indirectly inhibits myosin II activity by directly inhibiting the Rho kinase ROCK (Uehata *et al*, 1997). Blebbistatin specifically inhibits the ATPase of myosin II directly (Straight *et al*, 2003). Either Y-27632 or blebbistatin inhibited cytokinesis (data not shown), but did not induce misorientation of the spindles (Figure 6A), indicating that myosin II is not involved in this mechanism. Recent studies have shown that myosin X, a member of the unconventional myosin family (Berg *et al*, 2000; Zhang *et al*, 2004), plays an

important role in nuclear anchoring to the cell cortex by linking microtubules and actin cytoskeleton in *Xenopus* oocytes (Weber *et al*, 2004). Then, we examined the role of myosin X by knocking it down with siRNA in HeLa-S3 cells on fibronectin (Figure 6B). We also examined the effect of downregulation of myosin IIA and/or myosin IIB on the spindle orientation (Figure 6B). The population of binucleate cells was increased in the cells transfected with myosin IIA

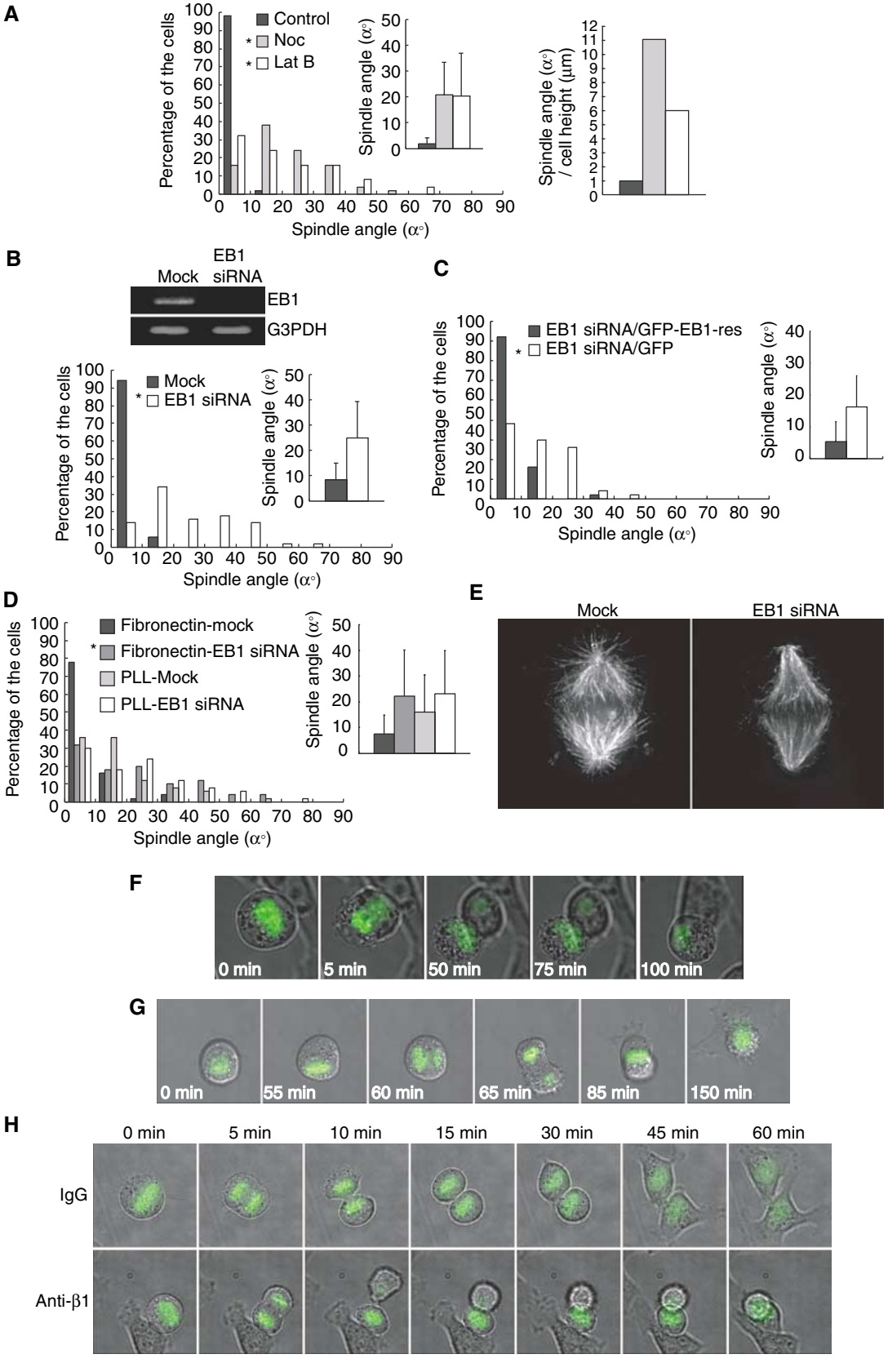

siRNA and myosin IIB siRNA, but not in mock, GFP siRNA, or myosin X siRNA-transfected cells (Figure 6C, left). In mock, GFP siRNA, and myosin IIA siRNA/myosin IIB siRNA-transfected cells, the spindles were properly oriented. In myosin X siRNA-transfected cells, however, the spindles were severely misoriented (Figure 6C, right). Essentially the same degree of the spindle misorientation was observed in HeLa-S3 cells transfected with the other myosin X siRNA, which targeted a different site of myosin X (Supplementary Figure S3). These results indicate that myosin X, but not myosin II, is required for proper spindle orientation in our system. Myosin X siRNA hardly changed the spindle length (1.9% increase) (Supplementary Figure S1G). The spindles were properly oriented in cells that spread to equal extents on fibronectin in mock cells, but misoriented in myosin X siRNA-transfected cells (Figure 6D), indicating that the effect of myosin X siRNA on spindle angle is not owing to indirect effects of spread basal area. Transfection of myosin X siRNA resulted in the misorientation of the spindle in the synchronized HeLa cells plated on fironectin for 10 h, but did not enhance the misorientation of the spindle in cells on poly-L-lysine (Figure 6E), suggesting that myosin X does not have an integrin-independent function in orientation of the spindle. Astral microtubules were normal in myosin X siRNA-transfected cells as compared with mock-treated cells (data not shown). Then, we examined the possible role of myosin X in actin reorganization during mitosis. HeLa-S3 cells had a number of stress fibers in prophase (data not shown). At the beginning of prometaphase, stress fibers disappeared and cortical actin structures appeared (Figure 6F, left, Mock, Prometa). At metaphase, cells round up, cortical actin structures became much more dense, and many retraction fibers were formed (Figure 6F, left, Mock, Meta). In myosin X-depleted cells, the actin structures were normal in prophase (data not shown), but the defects in actin organization became apparent in prometaphase and metaphase. The disappearance of stress fibers was delayed, and the attachment of the cells to the substrate surface was sustained (Figure 6F, left, MyoX siRNA, Prometa). Then, abnormal cell rounding (Figure 6F, left, MyoX siRNA, Meta, left, and Figure 6F, right) and the drastic reduction in cortical actin structures (Figure 6F, left, MyoX siRNA, Meta, right) occurred in metaphase. These defects in actin organization were not induced by the depletion of myosin IIA and myosin IIB (data not shown). These results clearly demonstrate that myosin X is necessary for actin reorganization during mitosis.

Discussion

Our results uncover a novel mechanism determining spindle orientation in nonpolarized cultured cells, which depends on integrin-mediated cell–substrate adhesion. This mechanism requires astral microtubules, actin cytoskeleton, the microtubule plus-end-tracking protein EB1, and myosin X. It should be noted that the spindle angles are lower in NRK cells than in HeLa cells (Figure 5A, Control). This may be due to the difference in the cell shape between these cell types. HeLa cells completely round up, whereas NRK cells remain flattened during mitosis. Thus, the geometrical constraints on the spindle orientation in NRK cells may lower the angles of misoriented spindles. It should be also noted that the spindle orientation is less perturbed by RGD peptides in NRK cells (Figure 3B), compared to HeLa cells. This discrepancy might be due to the difference in the classes of integrins that are expressed in these the cells. NRK cells might also express a subfamily member of integrin, which binds to fibronectin through the motifs other than RGD motif. The spindle orientation is perturbed by anti-β1 integrin antibody, but not by anti-β3 integrin or anti-αVβ6 integrin antibodies in HeLa cells. Our RT–PCR measurements could detect abundant expression of β1 integrin, but little, if any, expression of β3 integrin and β6 integrin in HeLa cells (data not shown). The specific requirement of β1 integrin for spindle orientation in HeLa cells might be due to its high level of expression in this cell line.

Disruption of actin cytoskeleton before or after the mitotic entry induces spindle misorientation (Figure 4A and B). However, the spindle orientation is less randomized in the cells treated with Lat B after mitotic entry (Figure 4B). In addition, after careful observations of time-lapse images of GFP-H2B-expressing HeLa cells, we realized that spindles were misoriented during spindle assembly and never aligned in most of the cells treated with Lat B before mitotic entry (Supplementary Movie 6 and data not shown). Therefore, some of the spindle alignment may occur during spindle assembly and it alters slightly if the actin cytoskeleton was disrupted after this event.

It has been reported that depletion of EB1 causes defects in the mitotic spindle structure, such as loss of astral microtubules, spindle shortening, and mispositioning of the spindle away from the cell center, in *Drosophila* S2 cells (Rogers *et al*, 2002; Goshima *et al*, 2005). Consistent with this report, we also observed the loss of astral microtubules and spindle

Figure 5 Astral microtubules and EB1 are required for the spindle orientation parallel to the substrate surface. (**A**) Synchronized NRK cells on fibronectin were treated with or without nocodazole (10 ng/ml) or Lat B (left), and subjected to the spindle orientation analysis (left, histogram; $n=50$, inset; mean ± s.d.; $n=50$). $^*P<0.005$, as compared with control, analyzed by *F*-test. The normalized values for the average spindle angle per the average cell heights were measured (right). (**B**) Asynchronous HeLa-S3 cells on fibronectin were transfected with or without EB1 siRNA, incubated for 72 h, and subjected to the spindle orientation analysis (bottom, histogram; $n=50$, inset; mean ± s.d.; $n=50$). $^*P<0.005$, as compared with the mock, analyzed by *F*-test. Total RNA was prepared and RNA levels of EB1 and control G3PDH were analyzed by RT–PCR (upper). (**C**) Synchronized HeLa cells on fibronectin were transfected with EB1 siRNA together with pEGFP or pEGFP-EB1-res. Cells were subjected to the spindle orientation analysis (histogram; $n=50$, inset; mean ± s.d.; $n=50$). $^*P<0.005$, as compared with the control pEGFP-transfected cells, analyzed by *F*-test. (**D**) Synchronized HeLa cells transfected with or without EB1 siRNA were plated on the coverslips coated with fibronectin or poly-L-lysine, incubated for 10 h, and subjected to the spindle orientation analysis (histogram; $n=50$, inset; mean ± s.d.; $n=50$). $^*P<0.001$, as compared with the mock, analyzed by *F*-test. (**E**) Mock-treated and EB1 siRNA-transfected HeLa-S3 cells were fixed and immunostained with α-tubulin antibodies. The images of a metaphase cell are shown. (**F**) Time-lapse images of the mitotic GFP-H2B-expressing HeLa cells on fibronectin, transfected with EB1 siRNA. The merge images of phase contrast and GFP-H2B are shown. (**G**) Time-lapse images of the mitotic GFP-H2B-expressing HeLa cells on fibronectin released from the nocodazole arrest. (**H**) Time-lapse images of the mitotic GFP-H2B-expressing HeLa cells that were plated on fibronectin in the presence of mouse IgG (IgG) or adhesion-blocking antibodies against β1 integrin (Anti-β1).

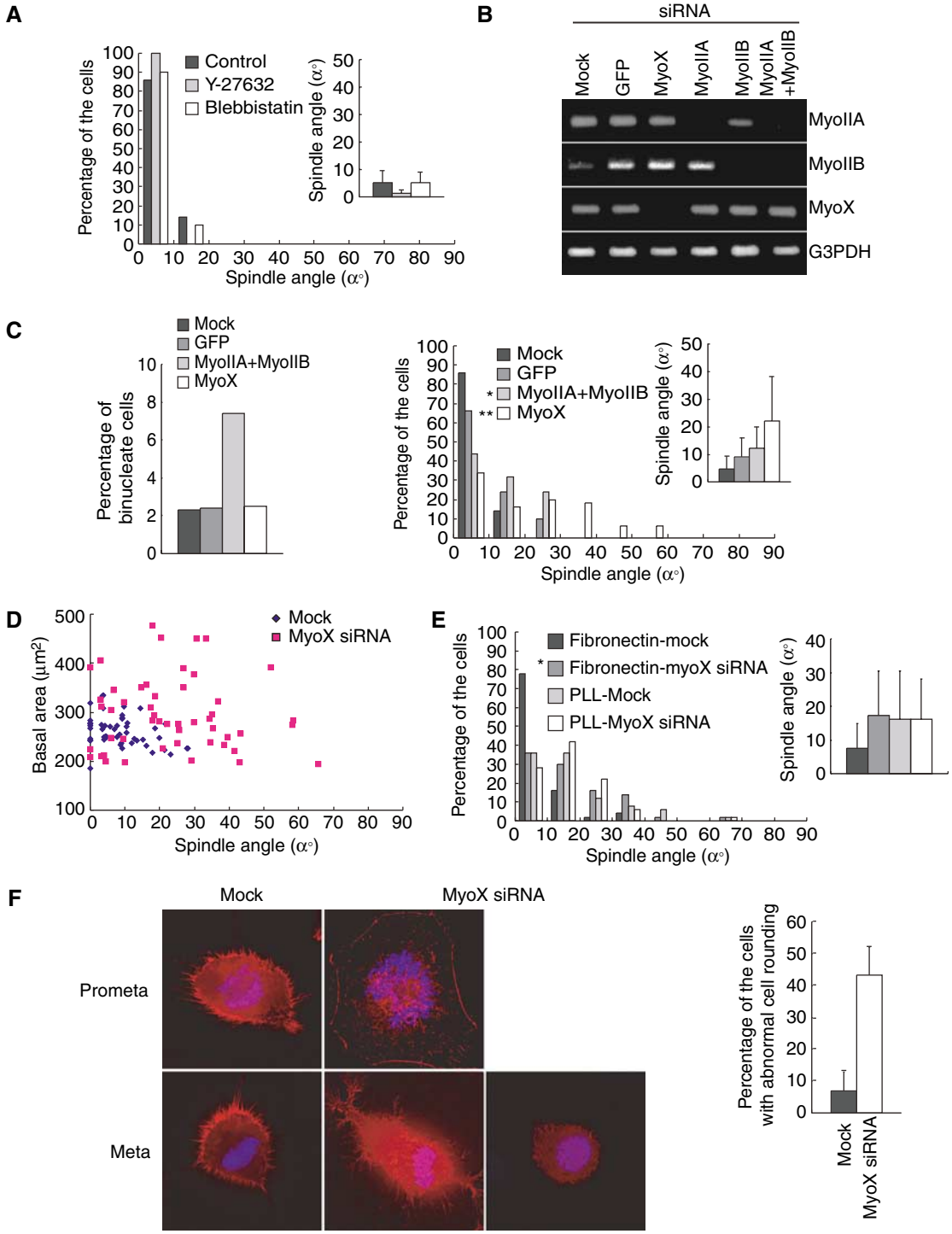

Figure 6 Myosin X is required for the spindle orientation parallel to the substrate surface and actin reorganization during M phase. (**A**) Synchronized HeLa cells on fibronectin were treated with DMSO (Control), Y-27632, or blebbistatin, and subjected to the spindle orientation analysis (histogram; $n=50$, inset; mean$\pm$s.d.; $n=50$). (**B**) Asynchronous HeLa-S3 cells on fibronectin were transfected with siRNAs for GFP, myosin X, myosin IIA, or myosin IIB, and incubated for 72 h. Total RNA was prepared and RNA levels of myosin IIA (first row), myosin IIB (second row), myosin X (third row), and control G3PDH (fourth row) were analyzed by RT–PCR. (**C**) Percentage of binucleate cells (left; $n>500$) and spindle orientation analysis (right; histogram; $n=50$, inset; mean$\pm$s.d.; $n=50$) in mock cells and in the cells transfected with GFP siRNA, myosin X siRNA, or myosin IIA siRNA and myosin IIB siRNA. $^{*}P>0.1$ and $^{**}P<0.001$, as compared with the GFP siRNA transfected cells, analyzed by *F*-test. (**D**) Spindle angles were plotted as a function of basal area in mock cells and in the cells transfected with myosin X siRNA ($n=50$). (**E**) Synchronized HeLa cells transfected with or without myosin X siRNA were plated on the coverslips coated with fibronectin or poly-L-lysine, incubated for 10 h, and subjected to the spindle orientation analysis (histogram; $n=50$, inset; mean$\pm$s.d.; $n=50$). $^{*}P<0.001$, as compared with the mock, analyzed by *F*-test. (**F**) Mock cells and the cells transfected with myosin X siRNA were fixed and stained with fluorescein-phalloidine (red) and Hoechst (blue) (left). Percentage of the metaphase cells with abnormal cell rounding was measured (right).

shortening in EB1 siRNA-treated HeLa S3 cells (Figure 5E and Supplementary Figure S1F), in which the spindle was not oriented parallel to the cell–substrate adhesion plane (Figure 5B). Moreover, we also frequently observed mispositioning of the spindle away from the cell center (data not shown) in EB1 siRNA-treated HeLa S3 cells. Thus, EB1 and astral microtubules may be required for both positioning of the spindle at the center of the cells and the correct orientation of the spindle parallel to the cell–substrate adhesion plane. Further studies will be required to determine whether spindle positioning at the center of the cells also depends on integrin-mediated cell–substrate adhesion. EB1 siRNA further enhanced spindle misorientation in HeLa cells even when the cells were plated on poly-L-lysine (Figure 5D). The function of EB1 in stabilization of astral microtubules might be independent of integrins and the loss of the astral microtubules–cortex interactions would destabilize the spindle axis in an integrin-independent manner.

Myosin II has been reported to be involved in centrosome separation and spindle assembly in PtK2 cells (Rosenblatt *et al*, 2004). In our hand, treatment of the cells with Lat B, the myosin II inhibitor blebbistatin or the ROCK inhibitor Y-27632 did not cause the defect in spindle assembly in HeLa cells (Supplementary Figure S4), even though these inhibitors efficiently inhibited cytokinesis (data not shown). This discrepancy might result from the difference in the requirement of myosin II for spindle assembly between PtK2 cells and HeLa cells. Proper spindle orientation in HeLa cells requires myosin X, rather than myosin II (Figure 6C). In budding yeast, a yeast homolog of EB1, Bim1, is shown to orient the spindle toward the bud, in cooperation with myosin (Myo2), in a microtubule-actin interaction-dependent manner (Gundersen and Bretscher, 2003; Pearson and Bloom, 2004). Thus, the molecular machinery regulating spindle orientation may be evolutionarily conserved in both polarized budding yeast and nonpolarized HeLa cells. It is reported that myosin X associates with microtubules and plays a role in nuclear anchoring to the cell cortex in *Xenopus* oocytes by linking microtubules and cortical actin (Weber *et al*, 2004). Therefore, myosin X could be acting like the yeast Myo2. However, the defects in actin reorganization, such as abnormal cell rounding and reduced cortical actin structures occur in metaphase in myosinX siRNA-transfected HeLa-S3 cells (Figure 6F). Therefore, we speculate that myosin X controls spindle orientation in an indirect manner in HeLa-S3 cells. We can hypothesize that myosin X may transport a hypothetical factor(s), which could have the ability to facilitate actin polymerization, from basal membranes to the cortex at the beginning of mitosis, and then would contribute to the assembly of cortical actin, which may be required for capture of astral microtubules. It is reported that myosin X transports integrins to facilitate cellular remodeling (Zhang *et al*, 2004). It is interesting to examine whether this myosin X-mediated transport of integrins plays some roles in spindle orientation.

The recent paper reported that the misorientation of mitotic spindles to the substratum leads to mitosis-associated detachment of cells from epithelial sheets, and may contribute to tumor dissemination in epithelial cells (Vasiliev *et al*, 2004). We show that one of the two daughter cells with misoriented spindles fails to maintain connection to the substratum after cell division in the cells treated with the anti-β1 integrin antibodies (Figure 5H and Supplementary Movie 10), transfected with EB1 siRNA (Figure 5F and Supplementary Movie 7), or in the cells released from nocodazole arrest (Figure 5G and Supplementary Movie 8). Therefore, the integrin-dependent mechanism for spindle orientation that orients the spindle along the axis parallel to the cell–substrate adhesion plane may ensure that both daughter cells remain attached to the substratum after cell division and prevent the mitosis-associated detachment of adherent cells from substratum.

While we were preparing this manuscript, Bornens group reported that the cell–substrate interaction through retraction fibers controls the planar orientation of the spindle along the *X/Y* plane on the substrate surface (Thery *et al*, 2005). Therefore, the planar spindle orientation and the spindle orientation parallel to the substrate surface are both shown to be dependent on cell–substrate adhesion. It will be interesting to examine how these two mechanisms are regulated coordinately.

Materials and methods

Cell culture, synchronization, and reagents

Cells were cultured and synchronized as described in Supplementary data. The following reagents are used: Lat B (Calbiochem); Y-27632 (Calbiochem); blebbistatin (CosmoBio); MG132 (Calbiochem); nocodazole (Sigma); aphidicolin (Sigma); GRADSP peptide (Calbiochem); GRGDNP peptide (Bachem); mouse IgG (Zymed); the antibodies against β1 integrin, β3 integrin, and αVβ6 integrin (Chemicon, clone 6S6, 25E11, and 10D5, respectively).

Cell staining and image analysis

The following antibodies and reagents were used for cell staining: α-tubulin (Sigma); γ-tubulin (Sigma); AlexaFluor 594-goat anti-mouse and 488-goat anti-rabbit IgG (Molecular Probes); rhodamine phalloidin (Sigma); DHCC (Sigma). Cells were stained and analysed as described in Supplementary data.

siRNA and rescue experiments

The siRNA of human EB1 and human β1 integrin were designed as described previously (Wen *et al*, 2004; Li *et al*, 2005). The siRNAs of human myosin X, myosin IIA, and myoin IIB were designed on the basis of the human myosin X, myosin IIA, and myoin IIB cDNA sequence, respectively, targeting to the region of nucleotides 628–646, 300–318, 1024–1042, respectively, counted from the start codon ATG. The siRNA of human myosin X in Supplementary Figure S3 was designed as described previously (Bohil *et al*, 2006). Annealed siRNAs were transfected by using Oligofectamine (Invitrogen). Media were changed to fresh medium 2 day after transfection and the cells were analyzed 72 h after transfection. For the siRNA experiments in synchronized cells, HeLa cells were transfected with the annealed siRNA for 6 h and then subjected to a double-thymidine block. For EB1 siRNA rescue experiments, we constructed pEGFP-EB1-res that was resistant to EB1 siRNA, by introducing four silent substitutions in the EB1 siRNA-target region. HeLa cells were transfected with pEGFP-EB1-res by using Lpofectamin Plus (Gibco-BRL), incubated overnight, and then transfected with EB1 siRNA by using Oligofectamine (Invitrogen). After 6 h incubation, cells were washed with fresh medium and subjected to a double-thymidine block.

Western blotting, RNA isolation, and RT–PCR analysis

To see the expression level of β1 integrin, cells were lysed in lysis buffer (20 mM Hepes pH 7.3, 25 mM 2-glycerophosphate, 50 mM NaCl, 1.5 mM $MgCl_2$, 2 mM EGTA, 0.5% Triton X-100, 2 mM DTT, 1 mM PMSF, 1 mM sodium vanadate, and 2 μg/ml aprotinin), centrifuged at 20 000 *g* for 15 min, and the supernatant was subjected to Western blotting analysis. To see the expression levels of EB1, myosin X, myosin IIA, myosin IIB, and G3PDH (control), total RNAs were isolated from the cells transfected with siRNAs by the use of RNeasy mini (Qiagen), and reverse-transcribed with random primers, followed by amplification with the primers designed specific for EB1 (5′-caaggtcaagaaactgcagtg-3′ and 5′-atactcttcttgctcctcctg-3′), myosin X (5′-atcttcgccatcgccaacgag-3′

and 5′-gttgttgtacacggtcttcgc-3′), myosin IIA (5′-gaagcagctcaagcggcagc tggag-3′ and 5′-ccgctttgccatctacctcttcgtc-3′), myosin IIB (5′-agcgacgcg tgccaacgcatctcgg-3′ and 5′-ggctgcgtctcgttgacatcactgg-3′), and G3PDH (5′-catccactggtgctgccaaggctgt-3′ and 5′-acaacctggtcctcagtgtagccca-3′).

Supplementary data

Supplementary data are available at *The EMBO Journal* Online (http://www.embojournal.org).

Acknowledgements

We thank H Saya for GFP-histone H2B expressing HeLa cells. We thank Y Mimori-Kiyosue for helpful discussion. We thank H Morimoto and K Mizoochi for technical assistance. This work was supported by grants from the Ministry of Education, Culture, Sports, Science and Technology of Japan (EN and FT) and PRESTO, JST (FT).

References

Berg JS, Derfler BH, Pennisi CM, Corey DP, Cheney RE (2000) Myosin-X, a novel myosin with pleckstrin homology domains, associates with regions of dynamic actin. *J Cell Sci* **113:** 3439–3451

Bienz M (2001) Spindles cotton on to junctions, APC and EB1. *Nat Cell Biol* **3:** E67–E68

Bohil AB, Robertson BW, Cheney RE (2006) Myosin-X is a molecular motor that functions in filopodia formation. *Proc Natl Acad Sci USA* **103:** 12411–12416

DeMali KA, Wennerberg K, Burridge K (2003) Integrin signaling to the actin cytoskeleton. *Curr Opin Cell Biol* **15:** 572–582

Geiger B, Bershadsky A, Pankov R, Yamada KM (2001) Transmembrane crosstalk between the extracellular matrix—cytoskeleton crosstalk. *Nat Rev Mol Cell Biol* **2:** 793–805

Goshima G, Wollman R, Stuurman N, Scholey JM, Vale RD (2005) Length control of the metaphase spindle. *Curr Biol* **15:** 1979–1988

Green RA, Kaplan KB (2003) Chromosome instability in colorectal tumor cells is associated with defects in microtubule plus-end attachments caused by a dominant mutation in APC. *J Cell Biol* **163:** 949–961

Gundersen GG, Bretscher A (2003) Microtubule asymmetry. *Science* **300:** 2040–2041

Gundersen GG, Gomes ER, Wen Y (2004) Cortical control of microtubule stability and polarization. *Curr Opin Cell Biol* **16:** 106–112

Hoffman DB, Pearson CG, Yen TJ, Howell BJ, Salmon ED (2001) Microtubule dependent changes in the assembly of microtubule motor proteins and mitotic spindle checkpoint proteins in PtK1 kinetochores. *Mol Biol Cell* **12:** 1995–2009

Kirschner M, Mitchison T (1986) Beyond self-assembly: from microtubules to morphogenesis. *Cell* **45:** 329–342

Kisselev AF, Goldberg AL (2001) Proteasome inhibitors: from research tools to drug candidates. *Chem Biol* **8:** 739–758

Lamprecht J (1990) Symmetric and asymmetric cell division in rat corneal epithelium. *Cell Tissue Kinet* **23:** 203–216

Li N, Zhang Y, Naylor MJ, Schatzmann F, Maurer F, Wintermantel T, Schuetz G, Mueller U, Streuli CH, Hynes NE (2005) Beta1 integrins regulate mammary gland proliferation and maintain the integrity of mammary alveoli. *EMBO J* **24:** 1942–1953

Lu B, Roegiers F, Jan LY, Jan YN (2001) Adherens junctions inhibit asymmetric division in the *Drosophila* epithelium. *Nature* **409:** 522–525

Machesky LM, Hall A (1997) Role of actin polymerization and adhesion to extracellular matrix in Rac- and Rho-induced cytoskeletal reorganization. *J Cell Biol* **138:** 913–926

Mimori-Kiyosue Y, Tsukita S (2003) 'Search-and-capture' of microtubules through plus-end-binding proteins (+TIPs). *J Biochem* **134:** 321–326

O'Connell CB, Wang YL (2000) Mammalian spindle orientation and position respond to changes in cell shape in a dynein-dependent fashion. *Mol Biol Cell* **11:** 1765–1774

Pearson CG, Bloom K (2004) Dynamic microtubules lead the way for spindle positioning. *Nat Rev Mol Cell Biol* **5:** 481–492

Pierschbacher MD, Ruoslahti E (1984) Cell attachment activity of fibronectin can be duplicated by small synthetic fragments of the molecule. *Nature* **309:** 30–33

Rappaport R (1996) *Cytokinesis in Animal Cells*. Developmental and Cell Biology Series 30. Cambridge: Cambridge University Press

Reinsch S, Karsenti E (1994) Orientation of spindle axis and distribution of plasma membrane proteins during cell division in polarized MDCKII cells. *J Cell Biol* **126:** 1509–1526

Robinson DN, Spudich JA (2004) Mechanics and regulation of cytokinesis. *Curr Opin Cell Biol* **16:** 182–188

Rogers SL, Rogers GC, Sharp DJ, Vale RD (2002) *Drosophila* EB1 is important for proper assembly, dynamics, and positioning of the mitotic spindle. *J Cell Biol* **158:** 873–884

Rosenblatt J, Cramer LP, Baum B, McGee KM (2004) Myosin II-dependent cortical movement is required for centrosome separation and positioning during mitotic spindle assembly. *Cell* **117:** 361–372

Schuyler SC, Pellman D (2001) Microtubule 'plus-end-tracking proteins': the end is just the beginning. *Cell* **105:** 421–424

Spector I, Shochet NR, Kashman Y, Groweiss A (1983) Latrunculins: novel marine toxins that disrupt microfilament organization in cultured cells. *Science* **219:** 493–495

Straight AF, Cheung A, Limouze J, Chen I, Westwood NJ, Sellers JR, Mitchison TJ (2003) Dissecting temporal and spatial control of cytokinesis with a myosin II Inhibitor. *Science* **299:** 1743–1747

Thery M, Racine V, Pepin A, Piel M, Chen Y, Sibarita JB, Bornens M (2005) The extracellular matrix guides the orientation of the cell division axis. *Nat Cell Biol* **10:** 947–953

Tirnauer JS, Bierer BE (2000) EB1 proteins regulate microtubule dynamics, cell polarity, and chromosome stability. *J Cell Biol* **149:** 761–766

Uehata M, Ishizaki T, Satoh H, Ono T, Kawahara T, Morishita T, Tamakawa H, Yamagami K, Inui J, Maekawa M, Narumiya S (1997) Calcium sensitization of smooth muscle mediated by a Rho-associated protein kinase in hypertension. *Nature* **389:** 990–994

Vasiliev JM, Omelchenko T, Gelfand IM, Feder HH, Bonder EM (2004) Rho overexpression leads to mitosis-associated detachment of cells from epithelial sheets: a link to the mechanism of cancer dissemination. *Proc Natl Acad Sci USA* **101:** 12526–12530

Wang JH, Manning BJ, Wu QD, Blankson S, Bouchier-Hayes D, Redmond HP (2003) Endotoxin/lipopolysaccharide activates NF-kappa B and enhances tumor cell adhesion and invasion through a beta 1 integrin-dependent mechanism. *J Immunol* **170:** 795–804

Weber KL, Sokac AM, Berg JS, Cheney RE, Bement WMA (2004) Microtubule-binding myosin required for nuclear anchoring and spindle assembly. *Nature* **431:** 325–329

Wen Y, Eng CH, Schmoranzer J, Cabrera-Poch N, Morris EJ, Chen M, Wallar BJ, Alberts AS, Gundersen GG (2004) EB1 and APC bind to mDia to stabilize microtubules downstream of Rho and promote cell migration. *Nat Cell Biol* **6:** 820–830

Wilson EB (1925) *The Cell in Development and Heredity*, 3rd edn. New York: The Macmillian Company

Yamada KM, Kennedy DW (1984) Dualistic nature of adhesive protein function: fibronectin and its biologically active peptide fragments can autoinhibit fibronectin function. *J Cell Biol* **99:** 29–36

Zhang H, Berg JS, Li Z, Wang Y, Lang P, Sousa AD, Bhaskar A, Cheney RE, Stromblad S (2004) Myosin-X provides a motor-based link between integrins and the cytoskeleton. *Nat Cell Biol* **6:** 523–531

